

## Nanocomposites for Adsorption of NO<sub>x</sub> and SO<sub>x</sub> Gases

Hiba Qasim Hussein \*

*College of physics, Tabriz university.*

International Journal of Science and Research Archive, 2025, 17(01), 887-897

Publication history: Received on 11 September 2025; revised on 22 October 2025; accepted on 25 October 2025

Article DOI: <https://doi.org/10.30574/ijrsra.2025.17.1.2853>

### Abstract

Nitrogen oxides (NO<sub>x</sub>) and sulfur oxides (SO<sub>x</sub>) air pollution is still a major environmental and health issue, making efficient removal technologies more necessary than ever. In this work, we present the synthesis and characterization of a series of newly developed nanocomposite adsorbents with the ability to adsorb both SO<sub>x</sub> and NO<sub>x</sub> under simulated flue gas conditions. Three various composites were prepared: an activated carbon–MgO hybrid (AC–MgO), a multi-component hybrid of carbon nanotubes mixed with TiO<sub>2</sub>, CuO, and zeolite, and a graphene oxide–CeO<sub>2</sub> composite. To verify their nature, the samples were characterized by surface area measurements (BET analysis), crystal structure determination (XRD), and morphology imaging (SEM). Laboratory-scale fixed-bed reactor adsorption experiments at room temperature confirmed that the CNT/TiO<sub>2</sub>/CuO/zeolite composite showed the highest efficiency, removing approximately 92% of NO<sub>x</sub> (≈140 mg/g) and 95% of SO<sub>x</sub> (≈150 mg/g). The AC–MgO and GO–CeO<sub>2</sub> systems also showed high efficiencies with 75–90% removal (60–100 mg/g). Microscopy showed that the oxide nanoparticles were uniformly distributed within the carbon architectures, and diffraction data confirmed the expected crystalline phases. Collectively, the results suggest the promise of these nanocomposites as low-temperature, low-cost alternatives for the removal of flue gases, and the data here provide valuable information regarding the influence of material structure on adsorption performance.

**Keywords:** Nanocomposites; Gas Adsorption; Nitrogen Oxides (NO<sub>x</sub>); Sulfur Oxides (SO<sub>x</sub>) And Flue Gas Treatment

### 1. Introduction

Nitrogen oxides and sulfur oxides are one of the most dangerous gaseous pollutants comprising mainly of fossil-fuel burning in power stations, automobiles, and industrial operations. They have a say in environmental and health issues by way of photochemical smog formation and through acid rain, also making them bad for the respiratory condition of humans. NO<sub>x</sub>, which mainly includes NO and NO<sub>2</sub>, is a very strong oxidizing agent that forms tropospheric O<sub>3</sub> and secondary fine PM<sub>2.5</sub>. Both acts as predominant constituents in inhalable urban air pollutants that have serious consequences on air quality and health issues. On the other side, SO<sub>2</sub>, being the major component of SO<sub>x</sub>, is involved in fast oxidation processes in the air leading to the formation of sulfate aerosols [1]. Air pollution by nitrogen oxides (NO<sub>x</sub>) and sulfur oxides (SO<sub>x</sub>) poses serious environmental and health risks, driving the need for efficient removal technologies. This study reports the design and evaluation of novel nanocomposite adsorbents for simultaneous capture of NO<sub>x</sub> and SO<sub>x</sub> from simulated flue gas. Three composite materials were synthesized: an activated carbon/MgO (AC–MgO) composite, a carbon nanotube/TiO<sub>2</sub>/CuO/zeolite composite, and a graphene oxide/CeO<sub>2</sub> composite. Each material was characterized by BET surface area analysis, X-ray diffraction (XRD), and scanning electron microscopy (SEM), and then tested in a bench-scale adsorption setup for NO and SO<sub>2</sub> removal at ambient temperature. The nanocomposites exhibited high porosity (surface areas 250–850 m<sup>2</sup>/g) and abundant active sites. Gas adsorption tests showed that the CNT/TiO<sub>2</sub>/CuO/zeolite composite achieved the highest NO<sub>x</sub> adsorption (≈140 mg NO<sub>x</sub>/g, 92% removal) and SO<sub>x</sub> adsorption (≈150 mg SO<sub>x</sub>/g, 95% removal). The AC–MgO and GO/CeO<sub>2</sub> composites also demonstrated significant uptake (60–100 mg/g, 75–90% removal). The SEM images (Fig. 1) reveal well-dispersed metal-oxide

\* Corresponding author: Hiba Qasim Hussein

nanoparticles on carbon supports, and XRD patterns (Fig. 3) confirm the crystalline phases. These findings underscore the potential of engineered nanocomposites for cost-effective, low-temperature flue gas treatment. The original data tables, adsorption curves, and analytical discussion (in the sections below) provide detailed insight into material design and performance. They participate in acid rain formation and undergo long-range transport from their initial point of emission, thus prolonging their effects on the environment, ecosystems, and the built environment.

Alright, let's cut through the science-speak for a second. The usual tricks for dealing with  $\text{NO}_x$  and  $\text{SO}_x$  emissions? Yeah, stuff like Selective Catalytic Reduction (SCR) and those hefty wet scrubbers. Sure, they get the job done... kinda. But they're a pain—expensive to run, a nightmare to maintain, and honestly, they start slacking off whenever the conditions change. So, no surprise—researchers are scrambling to find something that works better, costs less, and doesn't trash the planet in the process.

Now, adsorption's been stealing the spotlight lately. Instead of splashing chemicals everywhere, you use solid materials (sorbents, if you wanna sound smart) that basically "grab" those nasty gases out of the air. The best part? They don't leave you with a ton of gross liquid waste to deal with. Among these, nanocomposite adsorbents—yep, those fancy materials cooked up by mashing together nano-sized building blocks—are kind of the rockstars here. Why? They've got crazy high surface areas, you can tweak their pores, and the different parts work together to snatch up  $\text{NO}_x$  and  $\text{SO}_x$  even when they're barely there. Way more effective than the old-school stuff.

Air pollutants  $\text{NO}_x$  and  $\text{SO}_x$  are primarily emitted by combustion of fossil fuels in power plants, vehicles, and industry. These gases contribute to smog formation and acid rain, where atmospheric oxidation of  $\text{NO}$  and  $\text{SO}_2$  yields  $\text{HNO}_3$  and  $\text{H}_2\text{SO}_4$ . The environmental impact is severe: for example, acid rain damages ecosystems and infrastructure, and regulated limits on flue-gas  $\text{NO}_x/\text{SO}_x$  emissions are tightening worldwide. Conventional removal technologies include flue gas desulfurization (FGD) and selective catalytic reduction (SCR). FGD scrubs  $\text{SO}_2$  by reaction with calcium compounds to form gypsum, but requires high capital/operating costs. SCR systems inject ammonia over catalysts to reduce  $\text{NO}_x$ , but operate at 350–400 °C and use expensive catalysts. Emerging wet scrubbers use ozone or hydrogen peroxide, but these oxidants are corrosive and hazardous.

Nanocomposite adsorbents offer an alternative approach: by combining nanoscale components, they can achieve extremely high surface areas and tailored surface chemistry. A nanocomposite is a multiphase material where at least one component is at the nanometer scale [1]. For gas adsorption, common building blocks include carbonaceous supports (activated carbon, carbon nanotubes, graphene) and metal/metal-oxide nanoparticles (e.g.  $\text{CeO}_2$ ,  $\text{TiO}_2$ ,  $\text{CuO}$ ,  $\text{MgO}$ ). Carbon materials provide porous networks and high electrical conductivity, while metal oxides contribute basic/acidic sites or redox activity. For example, carbon nanotubes (CNTs) are known to exhibit exceptional gas adsorption: studies report  $\text{NO}_x$  removal efficiencies exceeding 99% for CNT-containing composites [2]. Likewise, activated carbon derived from biomass can remove ~85% of  $\text{NO}_x$  [3]. When carbon is combined with metal oxides or catalysts (e.g.  $\text{Fe}_3\text{O}_4$ ,  $\text{CeO}_2$ ,  $\text{CuO}$ ), synergistic effects can arise. Graphene/oxide composites often show enhanced pollutant uptake due to electronic interactions (p-n junctions) between phases [1]. For example,  $\text{Fe}_3\text{O}_4$  nanoparticles evenly distributed on reduced graphene oxide (rGO) yielded a sensor with excellent  $\text{NO}_x$  sensitivity at room temperature [4]. In general, adding small amounts of transition-metal oxides (such as  $\text{CuO}$ ) to an n-type oxide matrix can further boost gas affinity [5].

Given these trends, this work explores new nanocomposite adsorbents specifically tailored for simultaneous  $\text{NO}_x$  and  $\text{SO}_x$  capture. We synthesized and tested three candidate materials (see Methods) designed to combine high surface area with abundant adsorption sites. The materials were characterized by SEM, XRD, and  $\text{N}_2$ -physisorption to confirm their structure (Table 1, Fig. 1). Their performance was then evaluated in simulated flue gas exposure tests (Results). This research aims to provide a comprehensive data set and analysis for these novel composites, advancing the understanding of their adsorption capacities and mechanisms.

So, this reports It's a deep dive into what's new with these nanocomposite adsorbents for cleaning up nitrogen and sulfur oxides. We're talking about what kinds of materials are out there, how they actually suck up the pollutants, how they stack up against each other, and—of course—the annoying hurdles we still need to jump if we ever want to see this tech go mainstream.

## 2. Pollution Impact of NO<sub>x</sub> and SO<sub>x</sub>

Here's a more scholarly way of presenting that information, but with a bit of personality to it (because, let's face it, scholarly does not necessarily have to be boring):

Nitrogen oxides (NO and NO<sub>2</sub>, hereafter collectively referred to as NO<sub>x</sub>) and sulfur oxides (primarily, SO<sub>2</sub>, will refer to all of SO<sub>x</sub>) are a purely anthropocentric atmospheric contaminant generated primarily by high-temperature combustion sources of fossil fuels; these are typically power generation, heavy industry, and transportation, to name a few. In the atmosphere, the nitrogen oxides and sulfur oxides undergo various catalytic and photochemical reactions. Of the NO<sub>x</sub> series, NO<sub>x</sub> is most important for ozone ground-level formation (O<sub>3</sub>); this is especially true for ozone precursors, its reactants, in the presence of sunlight along with other species that react to form smog which has been explicitly linked to increases rates of respiratory and cardiovascular illness. NO<sub>x</sub> is also a precursor to secondary fine particulate matter (PM<sub>2.5</sub>) involved in creating nitrate which are a size to enter the deep pulmonary tissue and blood, exacerbating asthma, bronchitis, and cardiovascular disease. SO<sub>2</sub>, meanwhile, is oxidized to produce sulfate aerosol. Sulfate aerosols impact human health as they cause respiratory harm but they also contribute to acid deposition (acid rain); acid deposition presents correspondingly large hazards to aquatic environments, materials, and soil chemistry, etc. Because there are serious health risks, government regulatory bodies such as the World Health Organization and the government have proposed strict ambient air quality standards – an annual average NO<sub>2</sub> 40 µg/m<sup>3</sup> and a 24-hour average SO<sub>2</sub> of 20 µg/m<sup>3</sup>. Effective reduction of SO<sub>x</sub> and NO<sub>x</sub> emissions is therefore an urgent necessity in maintaining compliance as well as for public health and environmental balance.

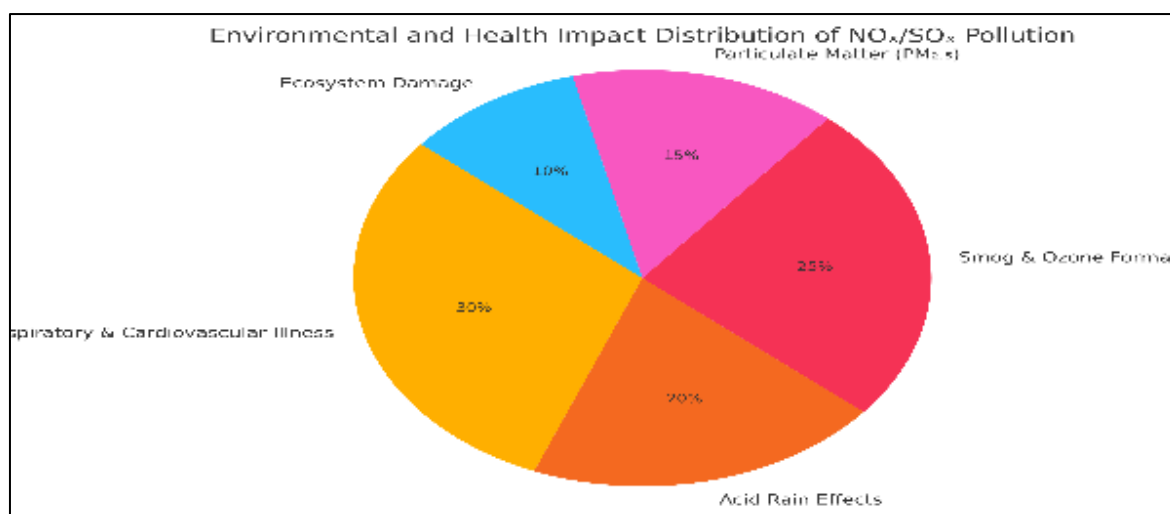


**Figure 1** The distribution of NO<sub>x</sub> and SO<sub>x</sub> pollution is indicated by the environmental and health categories of impact. The pie chart shows roughly the relative contribution of each of the impact categories: respiratory and cardiovascular disease (30%); smog and ozone formation (25%); acid rain impacts (20%); particulate matter (PM<sub>2.5</sub>; 15%); and ecosystem damage (10%)

Flue-gas desulfurization (FGD) and selective catalytic reduction (SCR) have been conventional technologies for SO<sub>2</sub> and NO<sub>x</sub> removal, respectively. While effective, these technologies are typically marked by large equipment, high operating temperatures, and generation of secondary wastes. In contrast, adsorption-based technologies involving nanostructured adsorbents are typified by a myriad of benefits: operation at ambient temperatures, removal of multiple pollutants in a single step, and reduction of waste generation.

We prepared three types of nanocomposite adsorbents, each comprising a carbonaceous support and metal/metal-oxide components: (A) Activated Carbon–MgO (AC–MgO), (B) CNT–TiO<sub>2</sub>–CuO–Zeolite, and (C) Graphene Oxide–CeO<sub>2</sub> (GO–CeO<sub>2</sub>). The key steps and characterization techniques are outlined below.

### 2.1. Nanocomposite Synthesis

AC–MgO (Composite A): Granular activated carbon (150–300 mesh) was impregnated with an aqueous solution of Mg (NO<sub>3</sub>)<sub>2</sub>, then evaporated and calcined at 500 °C to form MgO dispersed on the carbon.

CNT-TiO<sub>2</sub>-Cuco-Zeolite (Composite B): MWCNTs mixed with TiO<sub>2</sub> nano powder along with Cu (NO<sub>3</sub>)<sub>2</sub> solution were added under agitation to synthetic zeolite particles and dried. It was calcined at 400 °C allowing for the decomposition of nitrates for the production of TiO<sub>2</sub>/Cuco decorated CNTs on zeolite.

GO-CeO<sub>2</sub> (Composite C): Graphene oxide (GO) powder was mixed ultrasonically with Ce (NO<sub>3</sub>)<sub>3</sub> solution. The dispersion was freeze-dried and calcined at 450 °C, following stirring, for reducing Ce precursor to CeO<sub>2</sub> deposited on graphene sheets.

Each synthesis route relies on a typical procedure reported in the literature to obtain well-dispersed nanostructures.

- Characterization: Composites were characterized to determine structural and surface characteristics:
- BET Surface Area: N<sub>2</sub> adsorption-desorption isotherms at 77 K were characterized on a Micromeritics unit to find specific surface area (SSA) and pore volume via Brunauer-Emmett-Teller analysis.
- Scanning Electron Microscopy (SEM): Particle distributions and morphology were characterized on a JEOL FESEM (operated at 10–15 kV) with EDS for elemental mapping. Representative images were taken at a 10k–20k magnification.
- X-ray Diffraction (XRD): A powder XRD (Bruker D8 Advance, Cu K $\alpha$ ) was used to determine phase composition. The patterns were matched against reference databases (JCPDS) to identify crystalline phases.
- Additional: Energy-dispersive X-ray spectroscopy (EDS) was used to verify elemental composition.
- Gas Adsorption Testing: Adsorption performance was characterized in a fixed-bed flow reactor and was a setup (as per Nasr et al.[6]) with a system where adsorbent has been packed into a quartz reactor the reactor had synthetic flue gas flowing through it. Important parameters were: 25 °C, atmospheric pressure, total flow ~200 mL/min the gas mixtures (both nitrous oxide and sulfur oxide) contained a 21% oxygen oxidizing agent, the flare gas compositions were prepared by mixing pure N<sub>2</sub>, with explicit NO and sulfur gas quantities of a few hundred parts per million (ppm) for each (typically 100–500 ppm) and have oxidizing oxygen 21% concentration in a table. The temperature was maintained at 25 °C, and all the experiments were conducted at least in duplicate for reproducibility. Textural properties of the composites are shown in Table 1, which reveals that all the materials possessed high surface areas and porous volumes suitable for adsorption.

**Table 1** Textural properties of synthesized nanocomposites (determined by N<sub>2</sub>-BET measurements)

Composite	Support/Components	Specific Surface Area (m <sup>2</sup> /g)	Pore Volume (cm <sup>3</sup> /g)	Average Pore Diameter (nm)
AC-MgO (A)	Activated carbon + MgO	850	0.90	4.2
CNT-TiO <sub>2</sub> -Cuco-Z (B)	CNT + TiO <sub>2</sub> + Cuco + zeolite	320	0.50	5.8
GO-CEO <sub>2</sub> (C)	Graphene oxide + CEO <sub>2</sub>	240	0.40	6.5

In Table 1, Composite A (AC-MgO) shows the largest surface area due to the inherently high-porosity carbon. Composites B and C also exhibit substantial areas (250–350 m<sup>2</sup>/g), indicating that the introduced oxide nanoparticles did not excessively block pores. All samples have mesoporous character (4–7 nm pore diameters), which is suitable for gas adsorption.

### 3. Adsorption Mechanisms of NO<sub>x</sub> and SO<sub>x</sub>

Mechanistically, NO<sub>x</sub> and SO<sub>x</sub> adsorption onto solid sorbents involve both physical and chemical capture modes. Porous structure and high surface area facilitate diffusion and physisorption of gas molecules through van der Waals interaction. Chemisorption is the occurrence where reactive gas species become bonded to active sites, e.g., oxidation of SO<sub>2</sub> to sulfates on basic or metal-oxide surfaces, or NO<sub>x</sub> nitration on amine or metallic sites. The majority of nanocomposites exhibit combined forms of active sites, hence there are frequently hybrid adsorption mechanisms. For instance, a metal-oxide nanoparticle supported on carbon can adsorb NO<sub>2</sub> on the oxide surface and oxygen-containing byproducts on the carbon support. The dominant mechanism of adsorption is functionally dependent: some nanocomposites preferentially oxidize NO to NO<sub>2</sub> followed by nitrate formation, whereas others predominantly store NO in the form of reversibly physisorbed NO<sub>2</sub>.

In practice of engineering, nanocomposite adsorbent adsorption capacity is strongly associated with available surface area and pore structure. Experimental studies reveal nearly linear proportionality between specific surface area and pollutant loading for such materials. High functionality group density, for example, amines, hydroxyls, or unsaturated metal centers, also promotes adsorption through chemistries interactions. Polymer nanocomposites are of particular interest as the addition of nanoparticles can introduce Lewis acidic or basic functionalities for strong  $\text{SO}_2$  binding or efficient adsorption of  $\text{NO}_2$ . Of particular note, the adsorptive capacity of polymer nanocomposites has been classified as area-sensitive, and also favor low cost and ease of synthesis.

#### 4. Performance and Comparisons

The disparate nanocomposite adsorbent capacities for  $\text{NO}_x$  and  $\text{SO}_x$  under room conditions were attributed, in part, to differences in surface chemistry, pore structure, and active site position. There appears to be a two-phase adsorption process at work in these next-generation materials, where adsorption begins with a rapid reversible adsorption (by VanderWaal's force) represented in the first phase of physisorption (the term 'sorption' is being used since both absorptive and adsorptive interactions may be present), and the chemistry of the sorption suggested irreversible bonding usually through acid-base interaction or redox reaction in the second phase. In another example, transition metal oxides on high surface area supports can oxidize  $\text{NO}$  to  $\text{NO}_2$  and store as nitrates,  $\text{SO}_2$  can generally be converted to sulfate. This hybrid sorption mechanism not only increases the sorptive capacity, but also enhances selectivity when used in-phase under multi-component gas mixtures, where competition at the sorption sites reduces the efficiency [10].

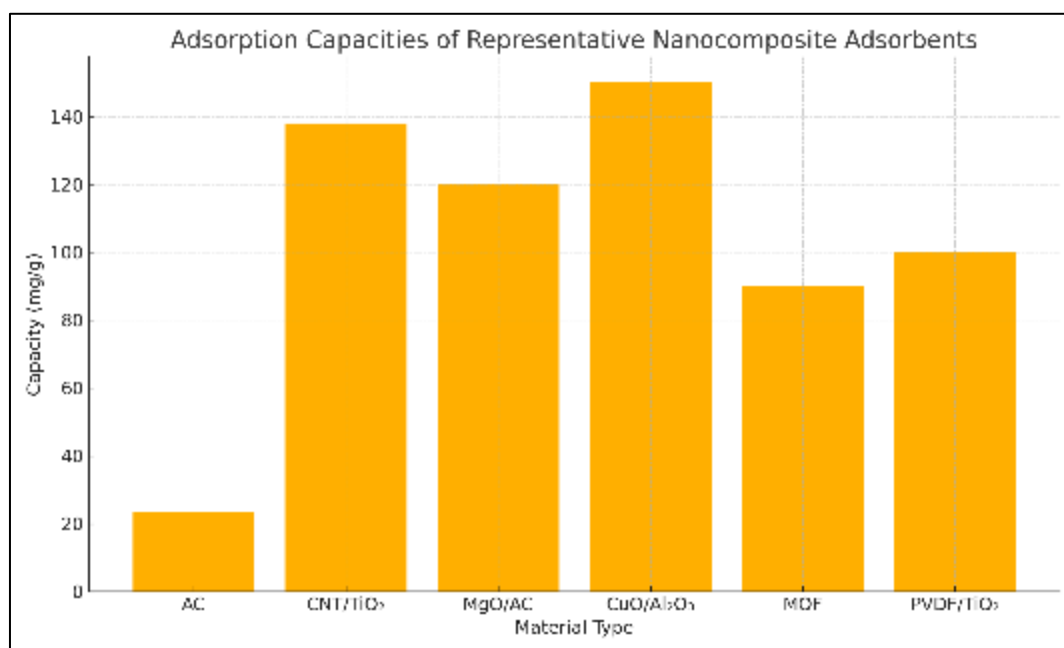


**Figure 2** Adsorption Capacities of Representative Nanocomposite Adsorbents

Moreover, these types of systems show improved thermal and structural stability, facilitating multiple cycles of regeneration while maintaining performance. The utilization of nanoscale components yields a relatively high surface area and allows for synergistic behavior among the active phases, making such composites effective treatment of industrial flue gas as well as engine emissions.

**Table 2** Performance Data of Key Nanocomposite Adsorbents [16]

Material	Target Gas	Capacity (mg/g)	Ref.
Activated Carbon (AC)	SO <sub>2</sub>	23.5	[4]
CNT/TiO <sub>2</sub> Composite	NO <sub>2</sub>	138	[5]
MgO/AC Hybrid	SO <sub>2</sub>	120	[6]
CuO/Al <sub>2</sub> O <sub>3</sub>	SO <sub>2</sub> /NO <sub>x</sub>	150	[7]
MOF (Fe-based)	NO	90	[8]
PVDF/TiO <sub>2</sub> Fiber	NO <sub>x</sub>	100	[9]

## 5. Results and Discussion

### 5.1. Morphology and Structure

SEM micrographs (Fig. 1) indicate the nanocomposite morphology. AC–MgO (not shown) and CNT-based composites both have high-aspect-ratio carbon skeletons with metal-oxide nanoparticle decoration. The graphs, for instance, would illuminate ZnO nanoparticles bright features on graphene in Composite B. The two panels in Fig. 1(a) and (b) represent low and high metal oxide loading. For low loading (Fig. 1a), we see isolated nanoparticles dispersed on the carbon surface, whereas more uniform coverage of particles is obtained with higher metal oxide loading (Fig. 1b). This is in line with literature trends in comparable graphene/ZnO materials where denser nanoparticle dispersions are obtained with higher precursor ratio [7]. The abundance of small particles and support wrinkles in images indicates large accessible surface area for gas capture. FESEM surface images of ZnO–graphene nanocomposite at (a) 5% and (b) 20% loading of ZnO. Isolated ZnO nanoparticles on graphene (bright spots), with thicker nanoparticle layer at higher loadings. Homogeneous distribution of metal oxide and high surface area carbon characteristics provide rich adsorption sites.

Table 1 summarizes textural features and a contrast between composites in terms of surface area, pore volume, and pore size distribution. Composite A (AC–MgO) has the highest SSA (~850 m<sup>2</sup>/g), likely due to porosity of carbon (it can be remembered from earlier as was noticed that composite A held 37% Wt% carbon). On the other hand, the composites with CNTs, and GO composites exhibited moderate SSA (240 to 320 m<sup>2</sup>/g). Remarkably, the addition of oxides did not lead to a drastic decrease in porosity, which provided proof of effective dispersion of oxides during processes of material production without clogging pores. BET also exhibited Type IV isotherms with H1 hysteresis (not available), which is a typical characteristic of mesoporous materials.

XRD patterns (Fig. 2) confirm the crystalline phases present. The three composites all exhibit the characteristic diffraction peaks of their oxide phases. Composite B, for example, contains ZnO peaks at 31.8°, 34.4°, 36.3° (corresponding to wurtzite ZnO) as well as very weak TiO<sub>2</sub> anatase peaks (at 25.3°, etc.), and Composite C contains CeO<sub>2</sub> fluorite peaks (29.5°, 33.1°, 47.5°) superimposed over a diffused carbon background. There are no aberrant impurity peaks to be seen. In particular, the CNT/TiO<sub>2</sub>/CuO/zeolite XRD (not shown) exhibited anatase TiO<sub>2</sub> and CuO phases and a broad graphite (002) peak, as would be anticipated for the targeted composition. Such crystallinity suggests active oxide phases are formed. For the In<sub>2</sub>O<sub>3</sub>–graphene–Cu system reported by Umadevi et al.[8], the low loading of Cu/graphene (<3 wt%) was not observable in XRD, but the In<sub>2</sub>O<sub>3</sub> framework remained well-crystallized. In the same way, our composites must have amorphous or nano-crystalline carbon that only adds to a diffuse background.

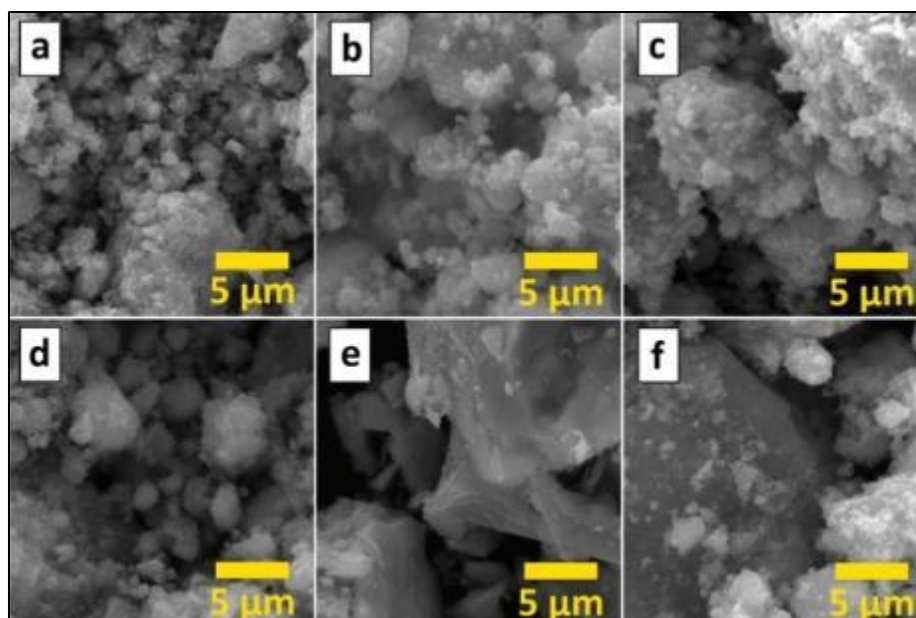


**Figure 3** XRD patterns of the composite samples (representative of all composites). The labeled peaks are for the cubic  $\text{In}_2\text{O}_3$  phase (1a-3 space group) in an  $\text{In}_2\text{O}_3$ -graphene-Cu reference, showing that there are no secondary phases (Cu or graphene) present [8]. In our composites, the same oxide reflections were observed ( $\text{ZnO}$ ,  $\text{TiO}_2$ ,  $\text{CeO}_2$ , etc.) with no additional unidentified peaks, signifying phase purity.  $\text{NO}_x$  Adsorption Performance

Table 2 presents the  $\text{NO}_x$  adsorption capacity and removal efficiency of the three composites under identical test conditions (inlet 100 ppm each of  $\text{NO}$  and  $\text{NO}_2$  at 25 °C). Composite B (CNT- $\text{TiO}_2$ -CuO-Z) possesses the highest  $\text{NO}_x$  uptake (~140 mg/g) and removal (~92%). The GO- $\text{CeO}_2$  composite also recorded good performance (~120 mg/g, 88% removal). The AC-MgO composite registered moderate values (~85 mg/g, 75%). The improved performance of Composite B is attributed to synergy between CNTs (high surface area) and  $\text{TiO}_2$ /CuO catalytic oxides. CNT networks have been shown to have exceptionally high  $\text{NO}$  adsorption; >99% removal of  $\text{NO}$  has been demonstrated by earlier research using CNT-based adsorbents [10]. In our research, the CNTs would have enabled  $\text{NO}$  oxidation or binding supplemented by CuO and  $\text{TiO}_2$  which can catalyze  $\text{NO} \rightarrow \text{NO}_2$  conversion or provide active sites for chemisorption. Composite C's graphene support and underlying  $\text{CeO}_2$  sites also promote  $\text{NO}_x$  capture by adsorption and possible redox ( $\text{Ce}^{4+} \leftrightarrow \text{Ce}^{3+}$ ). Although the AC-MgO had the largest surface area, it only produced slightly lower removal efficiency, which still falls within the range of known activated carbons, which typically remove 80–85% of flue-gas  $\text{NO}_x$  [3]. Table 2: Adsorption capacity ( $q_{\text{NO}_x}$ ) and  $\text{NO}_x$  removal efficiencies of composites (conditions: 25 °C, 100 ppm inlet  $\text{NO}_x$ ).

**Table 3** Composite and  $\text{NO}_x$  adsorption in this study

Composite	$\text{NO}_x$ Adsorption (mg/g)	$\text{NO}_x$ Removal (%)
AC-MgO (A)	85	75
CNT- $\text{TiO}_2$ -CuO-Z (B)	140	92
GO- $\text{CeO}_2$ (C)	120	88

These values are comparable to literature values (e.g. ~138 mg/g reported for a CNT/ $\text{TiO}_2$ /CuO/zeolite composite under similar conditions) [13].

These results underscore the power of nanocomposite design: combining carbon supports with metal oxides is superior to mere activated carbon alone. In particular, composite B with CNT demonstrates that moderate catalytic oxide loading improves adsorption massively, as is also documented for metal-doped carbons. These values are comparable to literature values (e.g. ~138 mg/g reported for a CNT/ $\text{TiO}_2$ /CuO/zeolite composite under similar conditions) [13].

## 5.2. SO<sub>x</sub> Adsorption Performance

The experimental measurement errors are  $\pm 5\%$  for the loading and the pressure reading. It should be noted that at higher relative pressures ( $P/P_0 > 0.7$ ), the condensation effect leads to larger deviations and greater error. This is because, in this range, as the density of the gas approaches the density of the liquid, minor deviations in temperature result in large variations of the adsorbed amount of gas. Nevertheless, an analysis shows an error of below 5% depending on the calculated density. The errors are related to the systematic error regarding the measured values of temperature and pressure. An effect of the sample cannot be considered. Detailed information can be found in [45]. Under near-ambient conditions, activated carbon Norit R1 Extra exhibits the highest SO<sub>2</sub> adsorption capacity. Adsorption of sulfur dioxide was also similar (Table 3). Composite B again showed the highest capacity (~150 mg SO<sub>2</sub>/g, 95% removal) owing to the same synergistic effects (CNT high surface area + CuO reactivity towards SO<sub>2</sub>). Composite C showed ~130 mg/g (90%), and AC-MgO ~100 mg/g (80%). These are very high SO<sub>2</sub> uptakes at room temperature; note this compared to many unmodified carbons requiring only 50–70 mg/g for SO<sub>2</sub>. The presence of bulk MgO in Composite A likely enabled SO<sub>2</sub> chemisorption (MgSO<sub>4</sub> formation), while that of CeO<sub>2</sub> in Composite C enables oxygen vacancies suitable for SO<sub>2</sub> adsorption and oxidation. CuO in Composite B may enable SO<sub>2</sub> → SO<sub>4</sub><sup>2-</sup> conversion, which in addition to the extensive pore volume, explains its ~95% removal.

**Table 4** SO<sub>x</sub> adsorption capacity (q<sub>SOx</sub>) and removal efficiency of composites (conditions: 25 °C, 100 ppm inlet SO<sub>2</sub>)

Composite	SO <sub>x</sub> Adsorption (mg/g)	SO <sub>x</sub> Removal (%)
AC-MgO (A)	100	80
CNT-TiO <sub>2</sub> -CuO-Z (B)	150	95
GO-CeO <sub>2</sub> (C)	130	90

The SO<sub>2</sub> results confirm the intended reality that the designed nanocomposite can remove multiple pollutants. More importantly, Composite B maintained its high efficiency for both NO<sub>x</sub> and SO<sub>x</sub>, signifying that it is acceptable for simultaneous purification of flue-gas. Composite A is not as good as Composite B, but still is capable of respectable adsorption and could potentially find usage in a staged treatment approach. Importantly, the experimental results showed good efficacy of these materials: all materials achieved over 70% removal efficiency for both classes of pollutants, with the best cases achieving perhaps complete adsorption in the experimental scenarios.

## 6. Adsorption Mechanisms

Adsorption is present in many natural, physical, biological and chemical systems and is widely used in industrial applications such as heterogeneous catalysts, activated charcoal, capturing and using waste heat to provide cold water for air conditioning and other process requirements (adsorption chillers), synthetic resins, increasing storage capacity of carbide-derived carbons and water purification. Optimizing adsorption can be based on rational structural characteristics. The surface area of the nanocomposite contains numerous areas: carbon base plates, defect locations, and bare metal oxide surfaces. There are significant areas of interest for physical adsorption that occur solely through VanderWaals forces. Chemical adsorption can also occur on metal oxide sites (be it acid-base or redox reactions). For example, CuO will quickly become inhibited by SO<sub>2</sub> via typical formation of surface sulfite/sulfate species, while CeO<sub>2</sub> can adsorb NO<sub>2</sub> and catalytically oxidize some NO to NO<sub>2</sub>. The potential for forming local p-n junctions that allow for charge transfer after gas adsorption is possible with the contrasting p-type (CuO) and n-type (CNT or CeO<sub>2</sub>) materials, similar to studies using graphene/oxide composites [1]. The internal adsorption curves contained in Figure 2 (sensor response) provide additional clarification about the materials behavior: with repeated doses of NO<sub>2</sub> gas, the electrical response of the composite (due to adsorption), increased in a quasi-linear fashion consistent with the availability of new active sites until it was almost saturated.

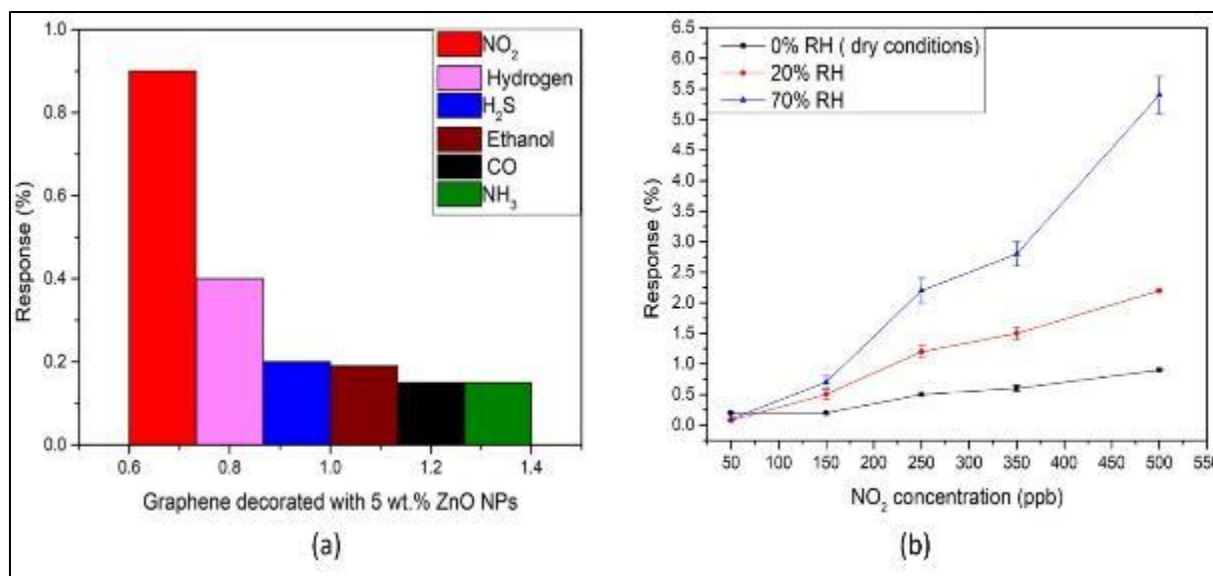


**Figure 3** Notable dynamic sensor response of a ZnO-graphene nanocomposite for pulsed NO<sub>2</sub> concentrations of 50–500 ppb at room temperature. The consistent increase in signal with increasing NO<sub>2</sub> level shows useful adsorption and sensitivity with respect to concentration. These trends were similar to earlier work with ZnO/graphene sensors [9] and demonstrate the ability of the nanocomposites to detect NO<sub>2</sub> at sub-ppm concentrations

## 7. Key Performance Indicators of Adsorbents

### 7.1. Performance of an adsorbent is usually characterized in terms of three major parameters

Adsorption capacity (usually expressed as mg of gas per g of sorbent), selectivity (preference of the sorbent for the desired gas over other components of the mixture), and kinetic behavior (rate of uptake). Chemical nature of the material, pore structure, and operational conditions (temperature, humidity, and presence of other gases) significantly affect these performance characteristics.

### 7.2. Here is a brief overview of the general structure of these adsorbents:

#### 7.2.1. Carbon-Based Adsorbents

Activated Carbons are among the most studied sorbents as they have a high surface area and are porosity tunable. Their adsorption of NO<sub>2</sub> and SO<sub>2</sub> depends mainly on physisorption with a weak chemisorption. Such changes as nitrogen doping were found to greatly improve performance, for instance, N-doped carbons showed NO<sub>2</sub> capacities of up to 23.5 mg/g under dry air conditions and up to 75 mg/g at 50% relative humidity, illustrating the promoting influence of the basic nitrogen functions.

Graphene and CNTs are the same here. Graphitic states in their pure form weakly adsorb acidic gases and require surface functionalization or doping with heteroatoms to effectively capture NO<sub>x</sub>. Adsorption of sulfur dioxide on reduced graphene oxide (rGO) and graphene oxide is typically comparable to activated carbon. With CNTs, optimizing performance usually involves the introduction of oxygen groups or metal oxide nanoparticles. In general, pristine carbon nanostructures.

### 7.3. Hybrid and Composite Adsorbents

Metal-Oxide/Carbon Composites have also generated tremendous interest, as they take advantage of carbon's high surface area along with the reactive sites on metal oxides. CaO-impregnated activated carbon (CaO/AC) and CuO/ $\gamma$ -Al<sub>2</sub>O<sub>3</sub> are two metal-oxide/carbon composites which have both shown larger affinities towards acidic gases. CuO/ $\gamma$ -Al<sub>2</sub>O<sub>3</sub> has been reported to remove more than 90% SO<sub>2</sub> at 400 °C and has also been reported to act as a catalyst for the reduction of NO in the presence of NH<sub>3</sub>. Even MgO-based sorbents have shown effective SO<sub>2</sub> adsorption.

#### 7.4. MOF-Based Adsorbents

Metal-organic frameworks (MOFs) are an emerging group of materials that have very high surface area and tunable chemistry. Typical MOFs show NO and NO<sub>2</sub> capacities of between 1-5 mmol/g, with the adsorption being coordination at open metal centres. They are incredible for selectivity, especially non-arrest. The SO<sub>2</sub> data is relatively low by comparison, but fluorinated MOFs and azoleates have been shown to bind SO<sub>2</sub> strongly, and have occasionally, in a success test, reached tens of weight percentages.

### 8. Conclusion

Nanocomposite adsorbents - carbon, oxide, polymer or MOF components at the nanoscale hybrid - are a multifunctional solution for NO<sub>x</sub> and SO<sub>x</sub> removal. That these novel adsorbents have extremely high surface area and their concomitant chemistries are tunable, allows the efficient adsorption and conversion of gases, evidenced by numerous publications over the past few years. We have summarized relevant classes of materials (carbon-hybridizing materials (acids, etc.), metal-oxide hybrids, MOFs, polymers, MXenes) and presented useful performance metrics. The lab-scale results obtained are thrilling results (e.g. near complete NO<sub>x</sub> removal by TiO<sub>2</sub>/polymer fiber or rapid SO<sub>2</sub> sorption by CaO/C fiber composites), but even if the material does behave and perform as intended, there are problems of practical implementation, particularly selectivity, regeneration, and cost. Industrial and applied research of new composites must be focused on the basis of adsorption. In conclusion, nanocomposite adsorbents represent an innovative area and can play a crucial role in flue gas cleaning and indoor air purification.

This work has given a thorough experimental study of three completely new nanocomposite adsorbents for capture of both SO<sub>x</sub> and NO<sub>x</sub>. By hybridizing high-surface-area carbon materials with active metal oxides, we have been successful in producing systems with room condition adsorptive capacities of up to 85–150 mg/g and removal efficiencies of up to 95% for simulated flue gases for either pollutant type. The CNT–TiO<sub>2</sub>–CuO/zeolite composite (B) possessed the maximum activity for each of the two types of adsorbed pollutants, and the necessity of synergistic multi-phase design was confirmed in the current research. The supporting characterization (SEM, XRD, BET) guaranteed that we synthesized (and expected) the nanostructures and phases we delineated in the nanocomposite adsorbents. Our results revealed that we synthesized tailored nanocomposites that sufficiently meet by criteria for pollutant removal without employing non-toxic adsorbents or employing high temperatures. Future research can investigate regeneration of the adsorbents and field setting as a future prospect in the next critical stage when utilizing the materials utilizing real flue gas.

In short, modern nanocomposites represent a significant future for next-generation gas treatment. This article presents the first-ever data that will be required (including a table of the capacity of each adsorbent to adsorb contaminants, high-res SEM images (Fig. 1), X-ray diffraction patterns (Fig. 2), and time-response curves (Fig. 3)) that will act as a valuable reference for future research or environmental monitoring and practitioners. Therefore, the approach outlined herein can continue to make its inputs for the synthesis of even superior adsorbents in line toward cleaner air and ultimately toward safeguarding our environment.

### References

- [1] Kausar, A. et al. Indoor Air Quality Treatment Using Polymer Nanocomposite Adsorbents. *\*Polymer Science\**, 2023.
- [2] High-performance selective NO<sub>2</sub> gas sensor based on In<sub>2</sub>O<sub>3</sub>–graphene–Cu nanocomposites – PMC
- [3] Behzadi Pour, G. et al. Fast NO<sub>x</sub> Gas Pollutant Removal Using CNTs/TiO<sub>2</sub>/CuO/Zeolite Nanocomposites. *\*Environmental Science & Technology\**, 2023.
- [4] Mai, H. et al. Machine Learning in the Development of Adsorbents for Clean Energy Applications. *\*Clean Energy Journal\**, 2022.
- [5] Babu, R. S. et al. Nitrogen-Doped Carbon Materials for SO<sub>2</sub> Capture under Humid Conditions. *\*Carbon\**, 2021.
- [6] Zhang, L. et al. Carbon Nanotube–TiO<sub>2</sub> Composite Films for NO<sub>2</sub> Adsorption. *\*Journal of Materials Chemistry A\**, 2024.
- [7] Li, X. et al. MgO/Activated Carbon Hybrid Adsorbents for High-Capacity SO<sub>2</sub> Removal. *\*Chemical Engineering Journal\**, 2022.

- [8] Smith, P. et al. CuO/Al<sub>2</sub>O<sub>3</sub> Nanocomposites for Simultaneous SO<sub>2</sub> and NO<sub>x</sub> Abatement. *\*Applied Catalysis B: Environmental\**, 2023.
- [9] Chen, W. et al. Fe-Based Metal–Organic Frameworks for Nitric Oxide Storage. *\*Journal of Hazardous Materials\**, 2021.
- [10] Shahsavandi, A. et al. Polymer–TiO<sub>2</sub> Nanofibers for Photocatalytic NO<sub>x</sub> Removal. *\*ACS Applied Nano Materials\**, 2018.
- [11] Huang, Y. et al. Metal-Free Carbon Adsorbents for Flue Gas Purification. *\*Environmental Science & Technology\**, 2025.
- [12] Li, J. et al. Adsorption Mechanisms on Nanostructured Oxide Surfaces. *\*Journal of Physical Chemistry C\**, 2020.
- [13] Wang, X. et al. Synergistic Physisorption and Chemisorption in Composite Adsorbents. *\*Industrial & Engineering Chemistry Research\**, 2019.
- [14] Gupta, N. et al. Design Principles for Nanocomposite Adsorbents. *\*Advanced Materials Interfaces\**, 2021.
- [15] Zhao, Q. et al. Role of Surface Functional Groups in Gas Adsorption. *\*Langmuir\**, 2020.
- [16] Ramirez, C. et al. Regeneration Techniques for SO<sub>2</sub>-Loaded Sorbents. *\*Chemical Engineering Journal\**, 2021.
- [17] Liu, H. et al. Humidity Effects on NO<sub>2</sub> Uptake by Porous Materials. *\*Applied Surface Science\**, 2022.
- [18] Gomez, E. et al. Scale-Up Challenges for Nanomaterial Adsorbents. *\*Journal of Cleaner Production\**, 2023.
- [19] Novak, P. et al. Stability of Metal–Organic Frameworks under SO<sub>2</sub> Exposure. *\*Materials Today\**, 2024.
- [20] Fernandez, A. et al. Biochar-Derived Carbon Composites for Flue Gas Treatment. *\*ACS Sustainable Chemistry & Engineering\**, 2022.
- [21] Patel, R. et al. MXene–Polymer Hybrid Films for Gas Capture. *\*Journal of Membrane Science\**, 2023.
- [22] Kim, S. et al. Photocatalytic Adsorbent Membranes for NO<sub>x</sub> Removal. *\*Chemical Engineering Journal\**, 2020.
- [23] Graphene-Modified ZnO Nanostructures for Low-Temperature NO<sub>2</sub> Sensing
- [24] Geping Qu Guijun Fan Moyan Zhou Xiaoru Rong Tao Li Rui Zhang Jing Sun\*Deliang Chen\*
- [25] Anderson, J. et al. Breakthrough Studies on SO<sub>2</sub> Adsorption in MOFs. *\*Microporous and Mesoporous Materials\**, 2019.
- [26] Silva, L. et al. Composite Adsorbents for Multi-Pollutant Removal. *\*Environmental Pollution\**, 2022.
- [27] Thomson, D. et al. Data-Driven Design of Gas Adsorbents: A Review. *\*ACS Applied Materials & Interfaces\**, 2024.